Science Background for the Reprocessing and Goddard Satellite-based Surface Turbulent Fluxes (GSSTF2c) Dataset for Global Water and Energy Cycle Research

Version 1.0

Release Date: October 28, 2011
Updated Date: May 16, 2014

Goddard Earth Sciences Data and Information Services Center (GES DISC)
http://disc.gsfc.nasa.gov
NASA Goddard Space Flight Center
Code 610.2
Greenbelt, MD 20771 USA

Science Background for the Reprocessing and Goddard Satellite-based Surface Turbulent Fluxes (GSSTF2c) Dataset for Global Water and Energy Cycle Research

The global water cycle's provision of water to terrestrial storage, reservoirs, and rivers rests upon the global excess of evaporation to precipitation over the oceans. Variations in the magnitude of this ocean evaporation excess will ultimately lead to variations in the amount of freshwater that is transported (by the atmosphere) and precipitated over continental regions. The air-sea fluxes of momentum, radiation, and freshwater (precipitation – evaporation) play a very essential role in a wide variety of atmospheric and oceanic problems (e.g., oceanic evaporation contributes to the net fresh water input to the oceans and drives the upper ocean density structure and consequently the circulation of the oceans). Information on these fluxes is crucial in understanding the interactions between the atmosphere and oceans, the global energy and water cycle variability, as well as in improving model simulations of climate variations.

The GSSTF2c (Version 2c) dataset is an upgraded and improved version from the preceding GSSTF2b (Version 2b) dataset released in October 2010. The Special Sensor Microwave Imager (SSM/I) [on board of a series of Defense Meteorological Satellite Program (DMSP) satellites] Version-6 (V6) brightness temperature (Tb) used for the GSSTF2b production was recently found possessing "artificial" temporal trends that were mainly due to the drifts/trends in the Earth incidence angle (EIA) found among the SSM/I satellites (e.g., F08, F10, F11, F13, F14 and F15). An algorithm that successfully handles the EIA problem has therefore been developed and applied to produce a corrected version of SSM/I Tb, which is subsequently used for producing the GSSTF2c dataset.

Document maintained by *GES DISC Personnel*

Prepared by: Chung-Lin Shie (UMBC/JCET, Code 612.0)

Edited and approved by: Andrey K. Savtchenko

Dataset Provider: Goddard Earth Sciences Data and Information Services Center
Dataset Provider Address: Code 610.2, NASA Goddard Space Flight Center, Greenbelt Rd., Greenbelt, MD 20771, USA

Table of Contents

1. Introduction

This document provides basic information for using Goddard Satellite-based Surface Turbulent Fluxes Version 2c (a.k.a. GSSTF2c) Dataset products.

The GSSTF2c (July 1987-December 2008) consists of products generated for the focus on Global Water and Energy Cycle Research. The global water cycle's provision of water to terrestrial storage, reservoirs, and rivers rests upon the global excess of evaporation to precipitation over the oceans. Variations in the magnitude of this ocean evaporation excess will ultimately lead to variations in the amount of freshwater that is transported (by the atmosphere) and precipitated over continental regions. The air-sea fluxes of momentum, radiation, and freshwater (precipitation – evaporation) play a very essential role in a wide variety of atmospheric and oceanic problems (e.g., oceanic evaporation contributes to the net fresh water input to the oceans and drives the upper ocean density structure and consequently the circulation of the oceans). Information on these fluxes is crucial in understanding the interactions between the atmosphere and oceans, the global energy and water cycle variability, as well as in improving model simulations of climate variations.

2. Overview and Background

2.1 Product/Algorithm Objectives

The previous GSSTF datasets (GSSTF2: July 1987-December 2000; GSSTF2b: July 1987-December 2008) have been widely used by scientific communities for global energy and water cycle research, and regional and short period data analysis since their official releases in 2001 and 2010, respectively, via NASA GES DISC. The objective of this project is to continually produce a uniform and improved dataset of sea surface turbulent fluxes (i.e., latent heat flux, sensible heat flux and wind stress) derived from remote sensing data (SSM/I) and reanalysis (NCEP) that would continue to be useful for global energy and water flux research and applications. We are looking forward to serving the scientific communities with one more useful dataset in GSSTF2c.

2.2 Historic Perspective

Accurate sea surface fluxes measurements are crucial to understanding the global water and energy cycles. The oceanic evaporation that is a major component of the global oceanic fresh water flux is particularly useful to predicting oceanic circulation and transport. The past GSSTF products, i.e., GSSTF2 (Chou et al. 2003) and GSSTF2b (Shie et al. 2010a; Shie 2010a), have been widely used by scientific communities since their official releases. Our records (based mainly on website online retrievals or personal communications) indicate that numerous individuals or groups have used the GSSTF2 or GSSTF2b datasets for scientific research. There have been more than 222 GSSTF2- or GSSTF2b-related research studies published either in peer-reviewed journals (at least 99) or non-peer reviewed publications such as conference presentations/papers, books and chapters, theses, reports, etc (at least 123) by September 2011. The users ranging from government agencies to universities and institutes, from various countries have performed diversified scientific projects.

The previous GSSTF2b product consists of two "sub-datasets", i.e., Set1 & Set2. GSSTF2b-Set2 was produced by manually excluding certain SSM/I satellite retrievals (trends) of brightness temperature (Tb) that were believed to have subsequently caused the artificial trends found in the globally averaged latent heat flux (mostly post 2000) of GSSTF2b-Set1. Hilburn and Shie (2011) recently found that the drift in the Earth incidence angle (EIA) associated with the SSM/I sensors on the DMSP satellites has accounted primarily for the artificial trends of the SSM/I Tb. An algorithm properly handling the EIA drifting problem has also been developed by Hilburn and Shie (2011), and applied to produce a corrected version of SSM/I Tb, which is then used for reprocessing the bottom-layer (the lowest atmospheric 500 meter layer) precipitable water (WB), and subsequently producing the upgraded GSSTF2c dataset that, e.g., includes surface specific humidity (Qair) and latent heat flux (E or LHF). WB, Qair and E of GSSTF2c have been found genuinely improved, particularly in the trends post 2000 (Shie and Hilburn, 2011). More related discussions are presented in later sections.

In addition to the aforementioned applications of the corrected SSM/I Tb and the improved WB, the GSSTF2c production, similar to the GSSTF2b production, also uses the input datasets such as the SSM/I V6 surface/10-m wind speeds (U), total precipitable water (W), as well as the sea surface temperature (SST), 2-m air temperature (Tair_2m), and sea level pressure (Psea_level) of the NCEP/DOE Reanalysis-2 (R2), along with the Cross-Calibrated Multi-Platform (CCMP) ocean surface wind vector product (Atlas et al., 2009). More detailed info's on GSSTF2b can be found in Shie et al. (2009), Shie et al. (2010a), and Shie (2010a).

2.3 Data Product Characteristics

Unlike GSSTF2b with two sub-datasets "Set1" and "Set2", GSSTF2c (July 1987-December 2008) only possesses one “Combined” dataset based on one set of combination of individual satellite products. The GSSTF2c data are stored in HDF-EOS5 files.

The GSSTF2c daily fluxes have first been produced for each available individual SSM/I satellite tapes (i.e., F08, F10, F11, F13, F14 and F15). Then, the Combined daily fluxes are produced by averaging (equally weighted) over available flux data/files from various satellites. These Combined daily flux data are considered as the "final" GSSTF2c, and are stored, along with the individual satellite data, in this HDF-EOS5 collection. Data should be used with care and proper citations, i.e., properly indicating your applications with, e.g., "using the combined 2001 data file" or "using the 2001 F13 data file". The users may feel free to use the products of the Combined or the individual satellites with their own interests.

The MEaSUREs project at GES DISC, however, converted all data into HDF-EOS5 format and reorganized it into separate daily and monthly files, in a manner consistent with the on-going Earth Observing System (EOS) missions such as Aura, Aqua, and Terra. The monthly, seasonal and yearly climatologies are also in HDSF-EOS5 format, in separate files. As such, the daily files are now easily searchable and downloadable by data day.

The essential meaning of HDF-EOS5 is that the data are now in a standard “Grid” format. The GSSTF2c eight major variables are grouped into one grid, named “SET1”, and stored in one file. Further, the “minor” variable - total precipitable water - is also grouped together with the eight major variables in the corresponding SET1 grid. Thus the grid contains 9 variables. This organization is identical for all daily and monthly files, apart from the model reanalysis. The “common”, NCEP/DOE Reanalysis II, data are stored in separate files with one Grid containing the four “common” variables. The climatologies (monthly, seasonal, and yearly) also contain the SET1 grid, but in addition are also containing the four NCEP variables in a separate grid.

The “individual tapes” representing the individual SSM/I satellites are stored in separate collections and daily files, one day per file. They contain one grid that is named on the satellite name (F08, F10, F11, F13, F14, and F15). The grid contains the nine variables (8 major + 1 minor) that go into the computation of the final nine “combined” retrieved variables.

All data within these HDF-EOS5 are easily recognizable as 360x180 arrays, representing global map, at 1x1 deg grid cell size. The endianness of the remote storage and the users’ local machines become irrelevant. The concept of headers and offsets, typical for the binary format, disappears and all that matters are Grid and data field names that are very easy to list out using command line utilities.

This data organization results in 13 data types, with Short Names listed below. The Short Name is the first string in all filenames, and it is also stored inside the files as a global file attribute “ShortName”.

A. Daily:
There are total of eight (8) daily data types.

GSSTF
GSSTF_NCEP

GSSTF_F08
GSSTF_F10
GSSTF_F11
GSSTF_F13
GSSTF_F14
GSSTF_F15

1) GSSTF
It has 1 grid, "SET1". Every grid has 9 parameters, the 8 "major" plus the "minor" total precipitable water.

2) GSSTF_NCEP
It has one grid, "NCEP", with 4 parameters. The original were the "common" binary files, that is the NCEP/DOE Reanalysis II.

3) GSSTF_Fxx
These are the individual satellites, where Fxx is one of the following (F08, F10, F11, F13, F14, and F15). The HDF-EOS5 files have only one grid, which takes the name of the individual satellite. Every grid has 9 parameters, the 8 "major" plus the "minor" total precipitable water.

B. Monthly:

There are two Monthly data types in he5.
GSSTFM
GSSTFM_NCEP

1) GSSTFM
It has two (2) grids: SET1, and SET1_INT, where "**INT**" stands for **interpolated**[1]. Each of these has 9 (nine) parameters: the 8 "major" plus the "minor" total precipitable water.

[1]**Note:** The "SET1_INT" is an interpolated product of the "SET1". Our goal for producing and distributing this extra "interpolation" product is to provide users with an additional dataset possessing less grid points (boxes or cells) with "missing" values.

2)GSSTFM_NCEP
This is the "common" monthly NCEP/DOE Reanalysis II. It has one grid with four parameters.

C. Climatology

There are three (3) climatological data types: Monthly, Seasonal, and Yearly in HDF-EOS5:
GSSTFMC
GSSTFSC
GSSTFYC

The climatologies (monthly, seasonal, and yearly) also contain the SET1 grid, but in addition are also containing the four NCEP/DOE Reanalysis II variables in a separate grid, "NCEP".

Summary of All Data Types:

GSSTF

GSSTF_NCEP
GSSTF_F08
GSSTF_F10
GSSTF_F11
GSSTF_F13
GSSTF_F14
GSSTF_F15
GSSTFM
GSSTFM_NCEP
GSSTFMC
GSSTFSC
GSSTFYC

The file naming convention for the non-climatological HDF-EOS5 files produced at GES DISC for the GSSTF2c project is as follows:

ShortName.vv.yyyy.mm.dd.he5

Where:

- ShortName = one of the following Data Types:
  GSSTF
  GSSTF_NCEP
  GSSTF_F08
  GSSTF_F10
  GSSTF_F11
  GSSTF_F13
  GSSTF_F14
  GSSTF_F15
  GSSTFM
  GSSTFM_NCEP
  GSSTFMC
  GSSTFSC
  GSSTFYC

- vv = 2c for this release
- yyyy = data year
- mm= data month
- dd = start date for the data
- he5 = commonly accepted extension for HDF-EOS5 files.

Filename example for the daily "combined" turbulent fluxes retrieval, for November 1, 2000:
GSSTF.**2c**.2000.11.01.he5

Climatologies have slightly different file names that reflect the Month (for monthlies), the range of Months (for seasonal), and the range of years for which the climatology is built. The yearly climatology has one file only.

Example file name for Monthly climatology for November:

GSSTFMC.2c.Nov.1988_2008.he5

Example file name for seasonal climatology for September-November:

GSSTFSC.2c.Sep_Nov.1988_2008.he5

Each **SET1** grid (including interpolated, **SET1_INT**[2]) contains the following 9 science data fields:

[2]**Note:** Only the interpolated version (SET1_INT) of the climatology products (monthly, seasonal or yearly) has been distributed.

data_field_short_name	Data field long name (units)
"E"	'latent heat flux' (W/m**2)
"STu"	'zonal wind stress' (N/m**2)
"STv"	'meridional wind stress' (N/m**2)
"H"	'sensible heat flux' (W/m**2)
"Qair"	'surface air (~10-m) specific humidity' (g/kg)
"WB"	'lowest 500-m precipitable water' (g/cm**2)
"U"	'10-m wind speed' (m/s)
"DQ"	'sea-air humidity difference' (g/kg)
"Tot_Precip_Water"	'total precipitable water' (g/cm**2)

Each NCEP Grid contains the following 4 data fields:

Data field short name	Data field long name (units)
"SST"	'sea surface skin temperature' (C)
"Psea_level"	'sea level pressure' (hPa)
"Tair_2m"	'2m air temperature' (C)
"Qsat"	'sea surface saturation humidity' (g/kg)

3. Physics of the Problem

The Earth's climate is characterized by a myriad of processes that couple the ocean, land, and atmosphere systems. The global water cycle's provision of water to terrestrial storage, reservoirs, and rivers rests upon the global excess of evaporation to precipitation over the oceans. Variations in the magnitude of this ocean evaporation excess will ultimately lead to variations in the amount of freshwater that is transported (by the atmosphere) and precipitated over continental regions. The air-sea fluxes of momentum, radiation, and freshwater (precipitation – evaporation) play a very essential

role in a wide variety of atmospheric and oceanic problems. Information on these fluxes is crucial in understanding the interactions between the atmosphere and oceans, the global energy and water cycle variability, as well as in improving model simulations of climate variations. These fluxes are thus required for driving ocean models and validating coupled ocean–atmosphere global models. Surface measurements of these fluxes are scarce in both space and time, especially over the oceans and in remote land areas. The Comprehensive Ocean–Atmosphere Data Set (COADS) has collected the most complete surface marine observations since 1854, mainly from merchant ships (Woodruff et al. 1993). However, the air–sea fluxes and input variables based on COADS have serious spatial and temporal sampling problems plus measurement uncertainty. It is, therefore, desirable that long-term global datasets of these fluxes be derived either from satellite observations or general circulation models (GCMs). Indeed, satellite measurements nicely complement conventional data to provide or improve space/time estimates of many hydrologic parameters. Several efforts have been made to prepare datasets of ocean surface turbulent fluxes from satellite observations using bulk flux models. The SSM/I on board a series of DMSP satellites spacecraft has provided global radiance measurements (e.g., the brightness temperature, Tb) for sensing the atmosphere and the surface. A number of techniques have been developed to derive the turbulent fluxes using parameters such as the surface air humidity and winds inferred from the SSM/I radiances (e.g., Chou et al., 1997; Schulz et al., 1997; Kubota et al., 2002). The author would particularly reemphasize the importance of the recent finding of the EIA drifting problem among the SSM/I satellites, and the successful correction on the infected Tb's that has subsequently led to the genuinely improved WB, Qair, and E of GSSTF2c.

4. Retrieval Algorithms

4.1 Ancillary Data Requirements

Similar to the preceding GSSTF2b fluxes, the GSSTF2c fluxes are produced using the up-to-date and improved input datasets, i.e., the SSM/I V6 surface/10-m wind speeds (U) and total precipitable water (W), as well as the NCEP/DOE Reanalysis-2 (R2) SST, 2-m air temperature (Tair_2m), and sea level pressure (Psea_level). As aforementioned, the lately improved bottom-layer precipitable water (WB) that incorporates the corrected SSM/I Tb with proper adjustments to the EIA drifts (Hilburn and Shie, 2011) is particularly used for reprocessing the GSSTF2c product. WB derived from the SSM/I Tb following Schulz et al. (1993), along with W, is used to retrieve surface air (~10m) specific humidity (Qair) using the first two vertical EOFs of First Global Atmospheric Research Programme (GARP) Global Experiment (FGGE) IIb humidity soundings of six W-based climatic regimes over global oceans during December 1978–November 1979 (Chou et al. 1995 and Chou et al. 1997). Qair and Qsat (surface saturation specific humidity based on SST), SST, Tair_2m and U are eventually applied in the GSSTF bulk flux model/algorithm to produce the three air-sea turbulent fluxes, i.e., wind stress (τ or WST), sensible

heat flux (H or SHF), and latent heat flux (E or LHF). Moreover, the CCMP ocean surface wind vector is used to partition τ into the respective wind stress vectors, i.e., STu and STv.

4.2 Calibration and Validation

The SSM/I V4 surface wind speeds that carried a linear trend of 6% increase in a 13.5-year period (Xing 2006) were used for producing the earlier version GSSTF2. The SSM/I V6 product (also including total precipitable water W) in which the spurious wind speed trends were removed by Remote Sensing Systems (RSS) was used for producing GSSTF2b (Shie et al. 2009; Shie et al. 2010a; Shie 2010a), which is now also applied for the GSSTF2c production. Shie et al. (2009; 2010a) showed a generally consistent improvement in the surface wind speed from SSM/I V4 to V6 by comparing the daily V6 and V4 (combined F13 and F14) surface wind speeds with in situ observed wind speeds from the five field experiments in 1999, i.e., Kwajalein Experiment (KWAJEX), the Joint Air–Sea Monsoon Interaction Experiment (JASMINE), the buoy service in the North Pacific (MOORINGS), the Nauru'99 (NAURU99), and the Pan–American Climate Study in the eastern Pacific during 1999 (PACSF99). Statistics showed a commonly reduced root-mean-square and bias, and increased correlation coefficient from V4 to V6 in four of the five experiments, except for NAURU99.

The SSM/I W and WB that were used for retrieving Qair using the EOF method were found varied insignificantly from V4 (for producing GSSTF2) to V6 (for producing GSSTF2b) [Shie et al. 2010a; Shie 2010a]. The upgrading from V4 to V6 accounts for a slightly greater impact on WB than W based on the ratio of the bias (V6 minus V4) to the V4 mean. WB had a larger ratio (1.51%) than that of W (0.49%). The retrieved Qair and fluxes (E, H, and τ) of GSSTF2b (based on V6) and GSSTF2 (based on V4) were also validated against the observations retrieved from the aforementioned five experiments. Qair of GSSTF2b had a slightly better correlation, but slightly higher bias than that of GSSTF2, while each of the three fluxes of GSSTF2b generally performed better than GSSTF2 by holding a higher correlation with the respective observation.

As noted in Shie (2010b), GSSTF2b-Set2 was produced post GSSTF2b-Set1 by artificially excluding certain satellite retrievals that were believed responsible for the relatively large trend occurred in the globally averaged E of Set1 mostly post 2000. The positive trend in E for Set1 was found mainly due to a negative trend in Qair and WB that must be related to the trends found in the SSM/I Tb's whose Tb19v, Tb19h, Tb22v, and Tb37v channels were used for retrieving WB (see Equation 1 in Section 4.4). Hilburn and Shie (2011) recently found that the SSM/I Tb's trends were due primarily to the drifts found in Earth incidence angle (EIA) of the SSM/I satellites. They further developed an algorithm that properly corrected the SSM/I Tb's and genuinely removed the artificial trends. The detailed algorithm can be found in Hilburn and Shie (2011). GSSTF2c, an upgraded and improved version of GSSTF2b, has thus been produced using the corrected and improved Tb's. The promising improvement, particularly found in WB, Qair and LHF of GSSTF2c is addressed in more details in Section 4.3.

4.3 Quality Control and Diagnostics

Latent heat flux, E, of the newly produced GSSTF2c and the preceding GSSTF2b-Set1 & Set2, (based on the combined SSM/I F13 and F14) is validated against the available ship measurement from the Stratus Ocean Reference Station (20^{o}S, 85^{o}W) during 2001, 2005-2007. Figure 1 shows that latent heat flux of GSSTF2b-Set2 has a reduced positive bias (15.81 Wm^{-2}) than that of GSSTF2b-Set1 (23.33 Wm^{-2}), yet with a lower correlation coefficient (0.55) than Set1 (0.68). The lower bias of GSSTF2b-Set2 is attributed to the removal of the high-trend data, while the lower correlation coefficient is due to the increased missing data (i.e., the reduced data sample points) that is also caused by the removal of the high-trend data. Figure 2 shows that latent heat flux of the newly produced GSSTF2c using the corrected (trend improved) Tb genuinely improves with a lower bias (16.54 Wm^{-2}) than that of GSSTF2b-Set1, as well as maintains a slightly improved correlation (0.684) than GSSTF2b-Set1 (0.683). Overall, GSSTF2c possesses a favorable bias (comparable to Set2), and a favorable correlation coefficient (comparable to Set1).

Impact of the corrected SSM/I Tb on the newly produced GSSTF2c can be further demonstrated through the globally averaged (0-360^{o}E, 90^{o}S-90^{o}N) time series of WB, Qair, and LHF, respectively, from January 1988 to December 2008 (21 years). Time series of the three parameters of GSSTF2c are shown, along with those of GSSTF2b-Set1 and GSSTF2b-Set2, in Figure 3. Note that GSSTF2b-Set2 (in blue) possesses smaller trends than GSSTF2b-Set1 (in red) post 1998, while it is basically identical to Set1 prior to 1997. In Fig. 3a, WB of GSSTF2c (in green) shows a considerably smaller decreasing trend than GSSTF2b-Set1 post 2000, while GSSTF2c also shows a smaller decreasing trend than both GSSTF2b-Set1 & Set2 during 1988-1991 (as Set1 and Set2 are identical). The GSSTF2c also shows a promising improvement in WB (trend) compared to GSSTF2b-Set2 during 2008 since the individual retrievals involving F13 and F15 have been effectively improved. According to a linear regression, WB possesses negative trends of -5.65% and -2.44% from January 1988 to December 2008 for GSSTF2b-Set1 & Set2, respectively, while the negative trend significantly reduces to -0.92% for GSSTF2c. Fig. 3b shows that Qair possesses decreasing trends that are comparable to those of WB, but with a slightly smaller magnitude, since Qair depends mainly on WB, and partially on the SSM/I V6 W (total precipitable water produced by RSS), which was generally found with a much smaller, or negligible trend. [Special note: unlike the RSS-issued original/"raw" SSM/I V6 Tb without a trend treatment, the RSS-issued SSM/I V6 W must have been retrieved with certain proper treatment]. Qair has negative trends of -4.19% and -1.94% during 21 years for GSSTF2b-Set1 & Set2, respectively, while the negative trend genuinely reduces to -0.63% for GSSTF2c.

Note that latent heat flux, E, depends on a combined effect of wind speed (U) and Qsat-Qair that may lead to a more complex trend pattern than Qair or WB. However, E may be reasonably assumed as inversely dependent of Qair or WB. In Fig. 3c, GSSTF2c shows a genuinely smaller positive trend than GSSTF2b-Set1 post 2000, while GSSTF2c also shows a smaller positive trend than both GSSTF2b-Set1 and Set2 during 1988-1991. The GSSTF2c shows a trend improvement in E compared to GSSTF2b-Set2

during 2008. For the global average, E has positive trends of 23.45% and 15.93% from January 1988 to December 2008 for GSSTF2b-Set1 & Set2, respectively. The trend genuinely reduces to 11.13% for GSSTF2c. The magnitude of the positive trend of E is considerably larger than that of the negative trend of WB or Qair since E, as aforementioned, involves a nonlinear relationship between U and Qsat-Qair, or more accurately, among U, Qair, and Qsat. Any possible positive trend occurred in U, SST (Qsat), or combined, might play a multiplying or amplifying effect on the existing negative trend (even just a small magnitude) of Qair/WB, and result in a greater positive trend for E. Similar Tb impact on WB, Qair and E was also found by Shie and Hilburn (2011) for various domain averages, i.e., over the quasi-global region (0-360°E, 60°S-60°N) and the tropical Pacific region (130-270°E, 30°S-30°N).

In closing this section, we would like to quote the insightful "**Rice Cooker Theory**" by Shie (2010a), i.e., "**To produce a bowl of delicious 'cooked rice' (useful and trustworthy 'output product') depends not only on a fine and working 'rice cooker' ('model/algorithm'), but also on good-quality 'raw rice' (genuine and reliable 'input data')**" that has further confirmed and helped us better comprehend the crucial and positive impact of the corrected SSM/I Tb on the therefore improved GSSTF2c product, particularly in WB, Qair and E.

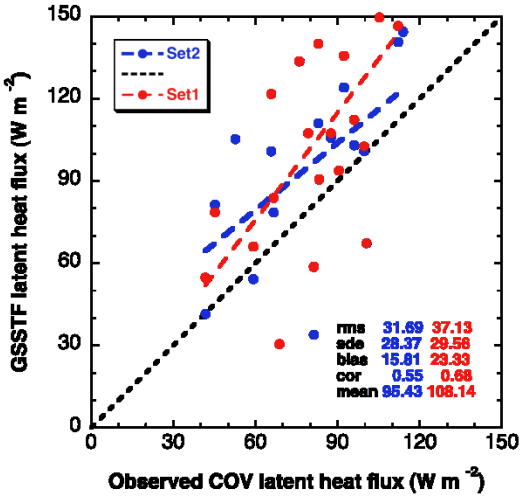

Figure 1: The GSSTF2b-Set1 (red solid circle) and GSSTF2b-Set2 (blue solid circle) daily latent heat flux (based on the combined SSM/I F13 and F14) vs. the available observations from the Stratus Ocean Reference Station (20°S, 85°W) during 2001, 2005-2007. Set1 has 22 data sample points, while Set2 has 16 sample points due to more missing data in Set2 than in Set1.

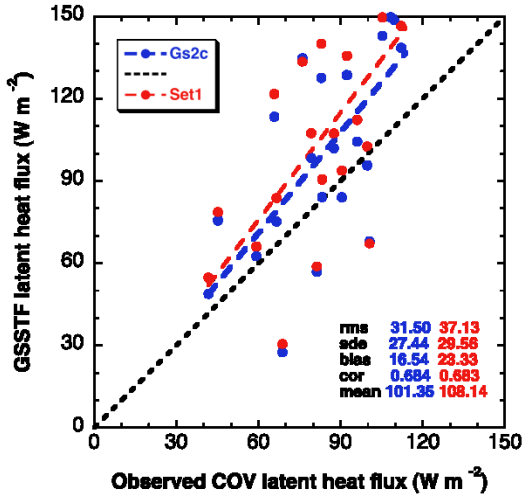

Figure 2: The GSSTF2b-Set1 (red solid circle) and GSSTF2c (blue solid circle) daily latent heat flux (based on the combined SSM/I F13 and F14) vs. the available observations from the Stratus Ocean Reference Station (20°S, 85°W) during 2001, 2005-2007. Both GSSTF2b-Set1 and GSSTF2c have 22 data sample points.

(a)

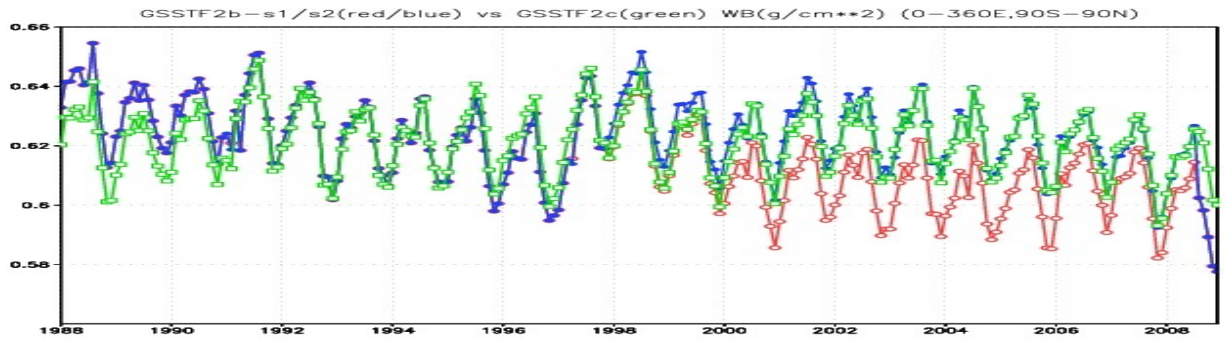

(b)

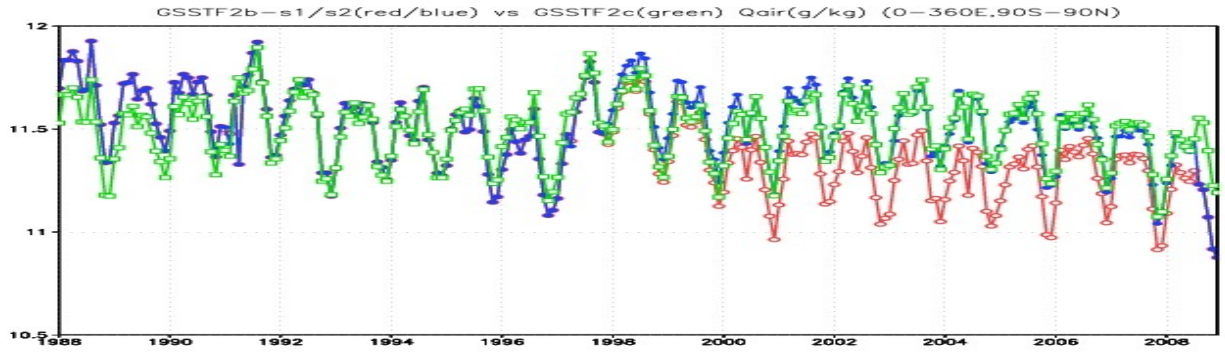

(c)

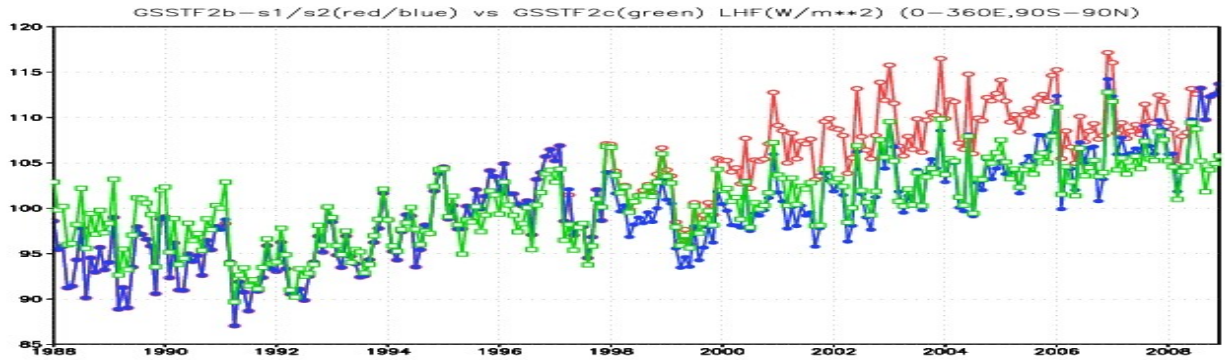

Figure 3: Time series of the globally averaged interpolated (a) WB (g cm^{-2}), (b) Qair (g kg^{-1}) and (c) E (W m^{-2}) for GSSTF2b-Set1 (in red), GSSTF2b-Set2 (in blue), and GSSTF2c (in green), respectively, from January 1988 to December 2008. Note that GSSTF2b-Set1 and GSSTF2b-Set2 are identical prior to 1997.

4.4 Algorithm Baseline Selection

The surface specific humidity Qair is retrieved from the instantaneous/daily total precipitable water W and bottom-layer precipitable water WB using an EOF algorithm (not shown here), while Qair depends highly on WB yet weakly on W (Chou et al.1995 and Chou et al. 1997). The daily WB is derived from the SSM/I Tb based on the WB-Tb relation (Schulz et al. 1993):

$$WB = b_0 + b_1\, Tb19v + b_2\, Tb19h + b_3\, Tb22v + b_4\, Tb37v, \quad (1)$$

where b_0, b_1, b_2, b_3, and b_4 are -5.9339, 0.03697, -0.02390, 0.01559 and -0.00497, respectively.

The GSSTF bulk flux model (based on the surface layer similarity theory, Chou, 1993) used for performing the GSSTF2c production is essentially the same as that for GSSTF2 (Chou et al. 2003) and GSSTF2b (Shie et al. 2010b). Similar to GSSTF2 and GSSTF2b, GSSTF2c requires the same methodology and same kinds of input data such as the surface/10-m wind speeds, total precipitable water, bottom-layer precipitable water, SST, 2-m air temperature, and sea level pressure. The air-sea turbulent fluxes, i.e., wind stress (τ), sensible heat flux (H), and latent heat flux (E) can be given in the following bulk aerodynamic formula:

$$\tau = \rho\, CD\, (U-Us)^2, \quad (2a)$$

$$H = \rho\, Cp\, CH\, (U-Us)\, (\theta s-\theta a), \quad (2b)$$

$$E = \rho\, L\upsilon\, CE\, (U-Us)\, (Qsat-Qair), \quad (2c)$$

where ρ is air density, Cp the isobaric specific heat, Lυ the latent heat of vaporization, CD, CH, CE the three respective bulk transfer coefficients, and Us is the negligibly small ocean surface current (about 0.55 of frictional velocity). The input parameters are the wind speed (U), the sea surface temperature (θs), the air potential temperature (θa), the specific humidity (Qair) at the reference height, and the saturation specific humidity (Qsat) at the sea surface temperature.

Based on surface layer similarity theory, the surface fluxes in Eqs. (1a)-(1c) can also be derived from the scaling parameters for wind or friction velocity (u∗), temperature (θ∗), and humidity (q∗) as

$$\tau = \rho\, u^{*2}, \quad (3a)$$

$$H = -\rho\, Cp\, u^*\theta^*, \quad (3b)$$

$$E = -\rho\, L\upsilon\, u^*q^*. \quad (3c)$$

For a given θs (or SST) and wind, temperature, and humidity at the measurement or reference heights within the atmospheric surface layer, the scaling parameters are solved through the roughness lengths and dimensionless gradients of wind, temperature, and humidity. The dimensionless gradients of wind, potential temperature, and humidity are functions of the stability parameter z/L, where z is the

measurement height, and L the Monin–Obukhov length, which depends on the scaling parameters or fluxes (detailed description can be found in Chou et al. 2003). Accordingly, the transfer coefficients, which reflect the efficiency of the vertical transportation of momentum, heat, and moisture flux, are a non-linear function of the vertical gradient in wind speed, temperature and water vapor near the surface and, therefore, are affected by the stability of the surface air. Liu et al. (1979) performed detailed analysis of the transfer coefficients based on their model and predicted that under low wind conditions the transfer coefficient might increase with increasing wind speed, because the increased roughness facilitates the transfer of heat and vapor. However, as the wind speed increases further, the sheltering effect due to the troughs between waves becomes more significant and will suppress the exchange of vapor and heat. As the wind speed reaches about 5 m s^{-1}, the negative and positive effects due to increased wind speed counterbalance each other. If wind speed increases further, the transfer coefficient may even start to decrease. Latest field and laboratory measurements have shown that the drag coefficient does not increase with wind speed at extreme wind conditions, i.e., greater than 30 m s^{-1} (Powell et al., 2003; Donelan et al., 2004). High-wind transfer coefficients (based on Powell et al., 2003; Donelan et al., 2004; Black et al., 2007) may be applied for the 10-m winds beyond 18 m s^{-1} (or even higher) in our future production of GSSTF3. Such a high-wind treatment may improve the surface flux retrieval, as well as provide a better understanding of weather systems with high winds such as tropical cyclones, hurricanes and typhoons.

5 Constraints, Limitations and Assumptions

Similar to the previous GSSTF products (e.g., GSSTF2b), the surface fluxes of GSSTF2c are limited to the global open-sea areas. Areas over continents/lands and the sea-ice covered oceans (i.e., high latitudes) are therefore filled with missing data.

As addressed earlier in Section 4, WB derived from SSM/I Tb, along with W, were used to retrieve surface air specific humidity (Qair) using the first two vertical EOFs of FGGEIIb humidity soundings of six W-based climatic regimes (Chou et al. 1995 and Chou et al. 1997). Two well-justified modifications/constraints applied in the GSSTF EOF algorithm for retrieving surface humidity (Chou et al. 1997) are worth mentioning:

(1) Over the wintertime extratropical oceans the SSM/I surface humidity retrieved by Chou et al. (1995) was systematically underestimated for Q < 5 g kg^{-1}. The reason for the negative humidity bias was that the surface humidity depended highly on WB that was underestimated for low WB < 3 kg m^{-2}. To reduce the negative humidity bias for the drier climatic regimes, the SSM/I surface humidity derived highly based on WB would be replaced by that derived mainly based on W if the latter was larger. This modification is restricted to the situation with W < 20 kg m^{-2} and WB < 2.8 kg m^{-2} for the wintertime extratropical oceans while excluding the trade wind belts.

(2) In the summer, as the warmer continental (or maritime) air moves over a colder ocean surface, fog or stratus may form with the surface air reaching saturation at a temperature near the underlying cold SST. These areas are generally located over the extratropical oceans and the cold oceanic upwelling regions off the west coasts of North America, South America, and Africa during the summer. Under this situation, the original EOF method of humidity retrieval (Chou et al. 1995) tended to overestimate the surface humidity when fog or stratus forms. To reduce the positive humidity bias, the saturation specific humidity (Qsat) of daily SSTs was used as an upper bound for the retrieval of SSM/I surface humidity.

In closing, we would like to reemphasize the importance of acquiring/using quality input datasets in the GSSTF flux production that is elaborated earlier via the quotation of the "Rice Cooker Theory" (Section 4.3). The recently improved SSM/I Tb, incorporating proper adjustments to the drifts in the Earth Incidence angle (EIA), has genuinely improved the quality of the retrieved WB, Qair and E of GSSTF2c. So does the authenticity of the input NCEP SST and Ta improve the quality of the retrieved H. Nonetheless, there should always be a room for us to further improve our future GSSTF flux product by acquiring further genuine and more reliable input datasets/parameters, as well as seeking a continual improvement/development in our GSSTF model/scheme.

6 Acknowledgement

This author C.-L. Shie, also the principal investigator (PI) of the lately revived GSSTF project, wishes to dedicate this GSSTF2c product to his mentor: the late research scientist S.-H. Chou (aka Sue). Without her genuine intelligence and intuition, great vision and perseverance, the productions of the newly upgraded GSSTF2c and the earlier revived GSSTF2b would have not been possible. Many thanks go to L. Chiu, R. Adler, I. Lin, E. Nelkin, and J. Ardizzone for their crucial contributions and supports right from the beginning of this project that have led to the successfully produced GSSTF2b and GSSTF2c, while a special thanks goes to K. Hilburn for his lately crucial contribution of successfully developing a useful algorithm properly resolving the Tb trends due to the drifts of EIA. The PI also owes a special thanks to A. Savtchenko for his precious help in converting the GSSTF2c (and the GSSTF2b previously) datasets from the original binary format into the HDF-EOS5 format for the official distributions via NASA GES DISC. A special thanks also goes to B. Vollmer and D. Ostrenga for their precious helps in the official distributions of GSSTF2c (and GSSTF2b previously). This study is supported by the MEaSUREs Program of NASA Science Mission Directorate-Earth Science Division. The PI is especially grateful to its program manager M. Maiden and program scientist J. Entin for their invaluable supports of this research.

7 References

Atlas R. M., J.V. Ardizzone, R. N. Hoffman, and J. C. Jusem, 2009: The cross-calibrated, multi-platform (CCMP) ocean surface wind product: Current status and plans. *The 2009 AGU Fall Meeting*, San Francisco, CA, December 14-18, 2009.

Black, P. G., E. A. D'Asaro, W. M. Drennan, J. R. French, P. P. Niiler, T. B. Sanford, E. J. Terrill, E. J. Walsh, and J. A. Zhang, 2007: Air-sea exchanges in hurricanes. *Bull. Amer. Meteor. Soc.*, 88, 357-374.

Chou, S.-H., 1993: A comparison of airborne eddy correlation and bulk aerodynamic methods for ocean-air turbulent fluxes during cold-air outbreaks. *Bound.-Layer Meteor.*, 64, 75-100.

Chou, S.-H., R. M. Atlas, C-L. Shie and J. Ardizzone, 1995: Estimates of surface humidity and latent heat fluxes over oceans from SSM/I data, *Monthly Weather Review,* **123**, 2405-2425.

Chou, S.-H., C.-L. Shie, R. M. Atlas, and J. Ardizzone, 1997: Air-sea Fluxes Retrieved from Special Sensor Microwave Imager Data, *Journal of Geophysical Research*, **102**, 12705-12726.

Chou, S.-H., E. Nelkin, J. Ardizzone, R. M. Atlas, and C.-L. Shie, 2003: Surface turbulent heat and momentum fluxes over global oceans based on the Goddard satellite retrieval, version 2 (GSSTF2). *J. Climate*, 16, 3256-3273.

Donelan M. A., B. K. Haus, N. Reul, W. J. Plant, M. Stiassnie, H. C. Graber, O. B. Brown, and E. S. Saltzman, 2004: On the limiting aerodynamic roughness of the ocean in very strong winds, *Geophys. Res. Lett.*, **31**, L18306.

Hilburn, K. A. and C.-L. Shie, 2011: Decadal trends and variability in Special Sensor Microwave Imager (SSM/I) brightness temperatures and Earth incidence angle. Report No. 092811, Remote Sensing Systems, 53 pp

Kubota, M., K. Ichikawa, N. Iwasaka, S. Kizu, M. Konda, and K. Kutsuwada, 2002: Japanese Ocean Flux Data Sets with Use of Remote Sensing Observations (J-OFURO). *J. Oceanogr.*, **58**, 213–215.

Liu W. T., K. B. Katsaros, and J. A. Businger, 1979: Bulk parameterization of air-sea exchanges of heat and water vapor including the molecular constraints at the interface. *J. Atmos. Sci.*, **36**, 1722–1735.

Powell, M. D. P. J. Vickery, T. A. Reinhold, 2003: Reduced drag coefficient for high wind speeds in tropical cyclones, *NATURE*, **422**, 279-283.

Schulz J., P. Schluessel, and H. Grassl, 1993: Water vapor in the atmospheric boundary layer over oceans from SSM/I measurements. Int. J. Remote Sens., **14**, 2773–2789.

Schulz, J., J. Meywerk, S. Ewald, and P. Schluessel, 1997: Evaluation of satellite-derived latent heat fluxes. *J. Climate*, **10**, 2782–2795.

Shie, C.-L., L. S. Chiu, R. Adler, E. Nelkin, I-I Lin, P. Xie, F.-C. Wang, R. Chokngamwong, W. Olson, and D. A. Chu, 2009: A note on reviving the Goddard Satellite-Based Surface Turbulent Fluxes (GSSTF) dataset. *Adv. Atmos. Sci.*, **26**, No. 6, 1071-1080.

Shie, C.-L., 2010a: A recently revived dataset of satellite-based global air-sea surface turbulent fluxes (GSSTF2b) – features and applications. *The 17th Conf. on Sat. Meteor. and Oceanog.*, 27 September – 1 October 2010, Annapolis, MD. (Keynote speech)

Shie, C.-L., L. S. Chiu, R. Adler, S. Gao, R. Chokngamwong, I-I Lin, E. Nelkin, J. Ardizzone, P. Xie, and F.-C. Wang, 2010a: A recently revived and produced global air-sea surface turbulent fluxes dataset – GSSTF2b: Validations and Findings. *Proceedings of the Joint 2010 CWB Weather Analysis and Forecasting & COAA 5th International Ocean-Atmosphere Conference*, 307-312, Taipei, Taiwan, June 28-30, 2010.

Shie, C.-L. and K. Hilburn., 2011: A satellite-based global ocean surface turbulent fluxes dataset and the impact of the associated SSM/I brightness temperature, *Proceedings of The 2011 EUMETSAT Meteorological Satellite Conference*, Oslo, Norway, September 5-9, 2011, 8 pp.

Woodruff, S. D., S. J. Lubker, K. Wolter, S. J. Worley, and J. D. Elm, 1993: Comprehensive Ocean-Atmosphere Data Set (COADS) release la: 1980–92. *Earth System Monitor*, **4**, 4–8.

Xing, Y., 2006: Recent changes in oceanic latent heat flux from remote sensing, Ph.D. Dissertation, School of Computational Science, George Mason University, Fairfax VA 22030, 119 pp.